ARTICLE IN PRESS

EDITOR'S CHOICE

Replication of Coupled Movements of the Wrist: A Cadaveric Study of Total Wrist Arthroplasty

Joanna Glanville, MBiolSci,*† Karl T. Bates, MPhil, PhD,* Natan Silver, MBChB,‡ Dileep Karthikappallil, MBChB,‡ Sebastiano Fichera, MSc, PhD,† Daniel J. Brown, MBChB, FRCS(Tr & Orth)*‡

Purpose The purpose of this study was to determine how well the active range of motion and the forces required to achieve motions are maintained following cadaveric implantation of the ball-and-socket style total wrist arthroplasty (TWA).

Methods An active wrist motion simulator was used to produce flexion, extension, radioulnar deviation, dart-thrower's motion, and circumduction in 14 fresh-frozen cadaveric wrists before and after TWA. Identical tendon displacements were applied to five major wrist flexors and extensors to control motion presurgery and postsurgery. Motion trials were recorded using biplanar video fluoroscopy and digitally reconstructed with 6 degrees of freedom using x-ray reconstruction of moving morphology. Wrist angles were subsequently measured with respect to an anatomically based radial coordinate system. Forces applied to the five actuated tendons were recorded by the simulator throughout all motion trials. Maximum wrist angles, dart-thrower's motion plane orientation, circumduction ellipse parameters, and peak tendon forces in pre-TWA and post-TWA conditions were compared.

Results There were no significant differences in maximal flexion, extension, radial, or ulnar deviation angles when comparing preoperative anatomic wrists with the same wrist following implantation of the TWA. Orientation of dart-thrower's motion planes and circumduction ellipses with respect to the sagittal plane increased after cadaveric surgery, whereas the area of the circumduction ellipses remained similar. Tendon forces were similar in anatomic and TWA wrists apart from flexor forces, which decreased in flexion in TWA wrists.

Conclusions In our cadaveric setup, the TWA was able to recreate functional motion patterns without significantly increased tendon forces.

Clinical relevance The results of this study support the assertion that a ball-and-socket style TWA can provide a postoperative range of motion adequate to perform activities of daily living. *(J Hand Surg Am. 2024;■(■):■−■. Copyright © 2024 by the American Society for Surgery of the Hand. Published by Elsevier Inc. This is an open access article under the CC BY license (http://creativecommons.org/licenses/by/4.0/).)*

Key words Motec, range of motion, tendon force, total wrist arthroplasty, wrist motion simulation.

Additional Material at jhandsurg.org

*From the *Department of Musculoskeletal & Ageing Science, Institute of Life Course & Medical Sciences, The William Henry Duncan Building, University of Liverpool, Liverpool, United Kingdom; the †School of Engineering, University of Liverpool, Liverpool, United Kingdom; and the ‡Liverpool Orthopaedic and Trauma Service, Liverpool University Hospitals, Liverpool, United Kingdom.*

Received for publication June 17, 2024; accepted in revised form December 4, 2024.

Corresponding author: Joanna Glanville, MBiolSci, Department of Musculoskeletal & Ageing Science, Institute of Life Course & Medical Sciences, The William Henry Duncan Building, University of Liverpool, Liverpool L7 8TX, United Kingdom; e-mail: hljglanv@liverpool.ac.uk.

0363-5023/24/■■-0001
https://doi.org/10.1016/j.jhsa.2024.12.006

Copyright © 2024 by the American Society for Surgery of the Hand. Published by Elsevier Inc. This is an open access article under the CC BY license (http://creativecommons.org/licenses/by/4.0/).

TOTAL WRIST ARTHROPLASTY (TWA) is a motion-preserving option for the treatment of end-stage arthritis of the wrist. In addition to relieving pain, it aims to maintain a functional range of motion (ROM), normally defined as a minimum of 5° flexion to 30° extension, with 10° of radial and 15° of ulna deviation,[1–4] and ideally 40° of both flexion and extension and 20° of both radial and ulnar deviation (RD and UD).[4] The study by Brumfield and Champoux[2] of normal and functional ROM of the wrist looked only at flexion and extension, whereas Ryu et al[4] also examined the second degree of freedom of radioulnar deviation; these sagittal and coronal plane movements are being described as "in-plane." Palmer et al[3] recognized a third degree of freedom consisting of carpal rotation, and Brigstocke et al[1] identified that many functional movements are combinations of in-plane movements, which they termed "coupled" movements. One specific coupled movement, from radial extension (RE) to ulna flexion (UF), the so-called dart-thrower's motion (DTM), has been thoroughly investigated and is now considered to be the primary functional movement of the wrist.[5,6]

Recent systematic reviews of TWA show that many reports of the outcomes do not detail post-operative ROM and those that do, predominantly report flexion-extension and radioulnar deviation arcs: DTM and circumduction have not been widely reported in the outcomes of TWA.[7,8] Furthermore, there is a suggestion that following TWA, movement is not as efficient as it is in the normal wrist with larger tendon forces needed to generate the same ROM.[9] This is presumably due to muscle moment arms around the wrist being altered after surgery, as has been seen in ball-and-socket-based replacements of other joints.[10,11] To date, research into tendon forces in TWA has only considered in-plane movements.[10]

The primary aim of the study was to analyze the active ROM of the wrist in all directions, in-plane, coupled, and out-of-plane (ie, occurring in an unintended plane), in the normal wrist and assess how well these movements are replicated following implantation of a Motec TWA (Swemac Innovations).[12] This research used an active wrist motion simulator to move cadaveric wrists, with biplanar videofluoroscopy to accurately measure the movement. The secondary aim was to determine how efficiently the TWA replicates the movement by analyzing the tendon forces that were required to generate the movement.

MATERIALS AND METHODS

Ethical approval for this study was granted by the University of Liverpool Central University Research Ethics Committee. Informed consent was obtained from all individuals prior to the donation of their body for scientific research.

Our hypothesis was that the TWA could accurately reproduce the ROM of the anatomic wrist. Normal flexion and extension of the wrist are stated as 60°.[4] We assumed a 10° decrease in flexion or extension to be the minimum change to be clinically significant (equating to a 16.67% decrease). The flexion-extension arc data from our validation study demonstrated a mean arc of 107.7° with an SD of 12.6.[13] With an α of 0.05 and powered at 95%, we estimated an appropriate sample size of 13 limbs.

To ensure the study was properly powered, we therefore studied 16 cadaveric wrists (distal humerus to fingertips), pre-TWA and post-TWA implantation, allowing for exclusions for technical issues if required. This included the raw data from six wrists that were analyzed as part of a pilot study that evaluated our cadaveric motion simulator.[13] Specimens originated from 10 donors aged 67–93 years (six men and four women); all were screened to confirm no radiographic premortem arthritis. Data from two wrists were excluded from the analysis, one due to the presence of midcarpal instability and the other due to incorrect implant placement and resultant breakage of a tendon suture. Fourteen wrists, pre-TWA and post-TWA, were included in the final analysis.

A programmable active wrist motion simulator that facilitates wrist kinematics to be studied using biplanar video fluoroscopy was designed and constructed and controls cadaveric wrist motion by displacing agonist tendons identically before and after a simulated surgery. A full description of its design and validation, for this and similar experiments, has been previously published.[13] The approach is summarized below, and the experimental setup is shown in Figure 1.[13]

Cadaveric limbs were mounted to the simulator such that fingertips pointed downward. Using a multilocked cruciate technique at the musculotendinous junction, 1.3 mm braided polyethylene sutures were attached to flexor carpi radialis, flexor carpi ulnaris, extensor carpi ulnaris, extensor carpi radialis brevis, and extensor carpi radialis longus. Sutures were passed through silicon tubes to exit the limb at the common flexor or extensor origin, as appropriate, to replicate their anatomical direction of action. The sutures were then attached to one of five individual units on the simulator, comprising a linear motor and encoder that control tendon displacement,

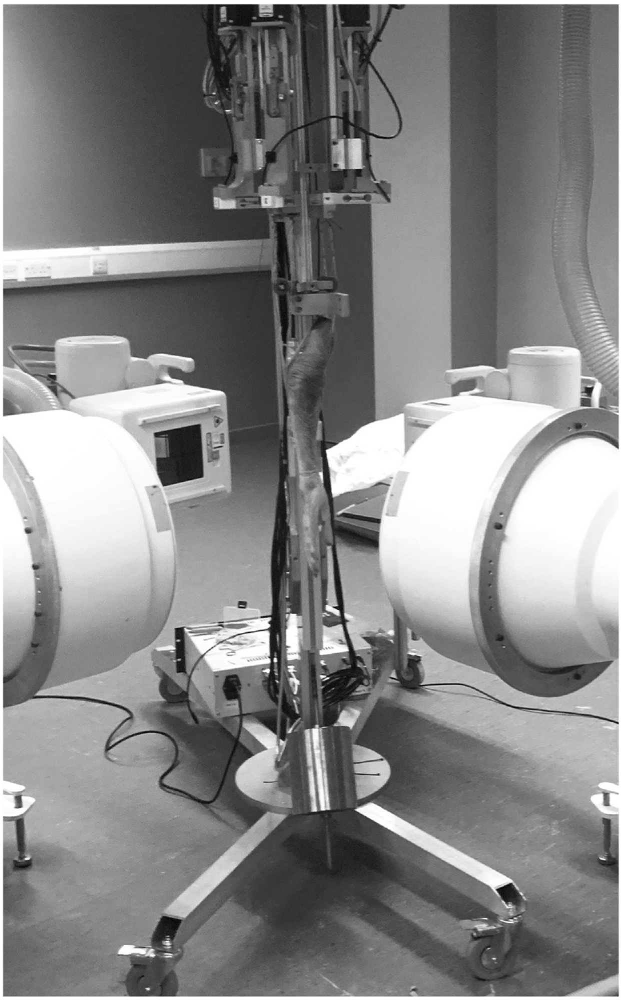

FIGURE 1: The experimental set up. A cadaveric forelimb is mounted on the active motion simulator. The wrist is positioned within the field of view of both x-ray cameras. This figure has been modified from Glanville et al.[13]

and a load cell that measures the force applied to the tendon. Prescribed displacement patterns, for each motion, were applied to each tendon to produce functional ranges of motion.[13]

To allow three-dimensional measurement of bone motion, three 1 mm diameter tantalum beads were inserted into the radius, ulna, capitate, second metacarpal (MCII) base, and third metacarpal (MCIII) head prior to data collection. A proximally-based capsulotomy was performed to insert the beads and then repaired. Biplanar video fluoroscopy, tendon force, and computed tomography data were then collected before and after the insertion of a TWA. In all cases, the previous capsular flap was reopened and repaired after insertion of the prosthesis. The insertion of the prosthesis was performed using the standard manufacturer's technique by, or under the supervision of, the senior clinical surgeon (Tang and Giddins[14] level 5). Biplanar fluoroscopy videos were captured for flexion, extension, RD, UD, and the components of DTM (RE and UF) at 50 fps and circumduction at 30 fps. Tendon force was sampled at 50 Hz. Three to five trials per motion were recorded after two warmup trials, and the initial wrist position was recorded in a static trial. Loads on all tendons were set to 2 N prior to a new motion.

ROM calculation

To reconstruct motion trials, bones and tantalum beads were segmented from the computed tomography scans using Mimics (version 25.0, Materialise). Subsequently, x-ray reconstruction of moving morphology techniques were used to create three-dimensional animations of radius, MCII and MCIII motion during every trial.[15,16] Radial coordinate systems were placed according to Akhbari et al,[17] with x axis being the long axis of the radius, y axis being the coronal interaction of the x axis and the distal radius articular surface, and the z axis being the sagittal cross-product of the x and y axes. The third metacarpal coordinate systems were also placed according to Akhbari et al[9] with the x-axis aligned with the MCIII diaphysis, the y-axis a best-fit line between the centroids of MCII, MCIII, and the fourth metacarpal, and the z-axis the cross-product of x- and y-axes.[9]

Wrist angles were defined as the position of the metacarpal coordinate systems with respect to the radial coordinate system and the zero position as the alignment of the two coordinate systems. For each motion in each specimen, mean angle was calculated in every frame to create angle profiles about each axis of the radial coordinate system. For all planar motions, angle profiles were truncated to finish at the point of maximum wrist excursion about the in-plane axis/axes or at the point before component impingement. The precise frame of impingement was taken as the point of a sudden increase in the tendon force curve gradient that corresponded to x-ray identification of impingement. Wrist ROM equaled the angles about the x, y, and z axes at the profile end point. Initial wrist position was determined for each motion by its respective static trial.

To visualize wrist motion paths graphically, x and y angle profiles were plotted against each other. Regression lines were fitted to the plotted RE and UF motion paths, and as the orientation of the DTM plane is functionally important, it was calculated as the angles between the RE and UF regression lines and the y-axis (sagittal plane).[18,19] Root mean

ARTICLE IN PRESS

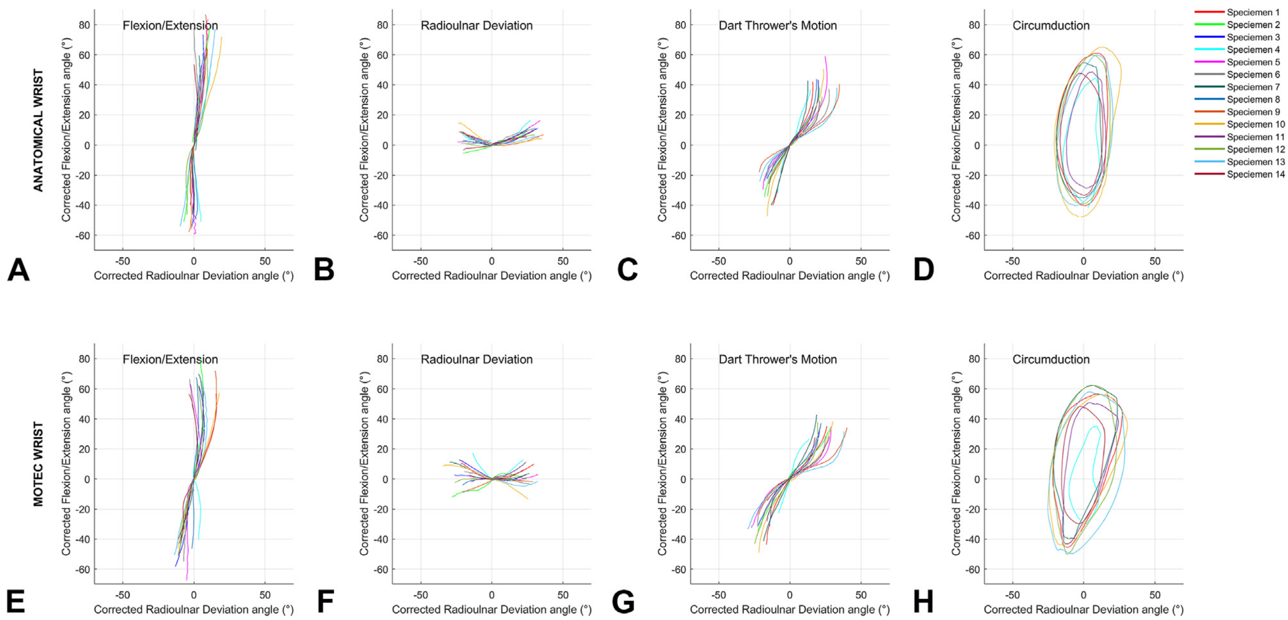

FIGURE 2: Wrist angle trajectories in individual specimens before and after TWA. Angles are reported about the flexion (+)/extension (−) and radial (−)/ulnar (+) deviation axes of the radial coordinate system and are corrected for individual start position (corrected ROM). Each trajectory represents an average of three to five trials. **A−D** Flexion-extension, radioulnar deviation, DTM, and circumduction in the anatomical wrist. **E−H** Flexion-extension, radioulnar deviation, DTM, and circumduction in the Motec wrist.

squared error between motion paths and regression lines determined the model's fit. An ellipse was fitted to the plotted circumduction envelope and the ellipse area, and orientation was calculated as an approximation of circumduction area and orientation. Ellipse fit was determined by root mean squared error calculated between the magnitudes of 100 vectors from the origin to the ellipse and the corresponding vectors on the circumduction envelope. To visualize mean wrist motion paths, truncated angle profiles of individual wrists were interpolated to 100 points. Mean wrist angles about the x- and y-axis at each of these points were plotted against each other.

Our workflow required us to set the starting positions of individual arms manually, which meant that anatomical starting angles were not standardized across individuals. As actuator displacements, and motion paths, are applied relative to these starting positions, it is useful for inter-specimen comparisons to additionally visualize motion paths after correction to account for differences in initial wrist position. This corrected ROM, calculated by subtracting the initial position from every sampling point in a wrist angle profile, allows the graphical representations of the ROM paths to have the same origin. Corrected ROM was only used graphically; all other results and statistics were generated using unmodified ("true") wrist angle profiles.

Tendon forces

Tendon forces were studied in four motion combinations, flexion/extension, radioulnar deviation, DTM, and circumduction. For each motion combination in each specimen, peak tendon forces across all trials were identified. Overall mean peak tendon forces were calculated for each motion.

Statistics

Statistical comparisons between anatomical and TWA wrists were performed. Shapiro-Wilk tests determined whether data were normally distributed. Then, either a paired-sample *t* test or Wilcoxon test determined whether initial/maximum wrist angles, DTM orientation, circumduction ellipse area/orientation, or tendon force differed significantly between the anatomic and TWA conditions. Significance was determined by a *P*-value below .05.

RESULTS

Initial wrist positions

Mean initial positions of pre- and post-TWA wrists are displayed in Table S1, available online on the *Journal's* website at www.jhandsurg.org. All motions commenced from a position of slight extension, and initial position did not vary significantly between pre- and post-TWA wrists ($P > .05$) (Table S1, available online on the *Journal's* website at www.jhandsurg.

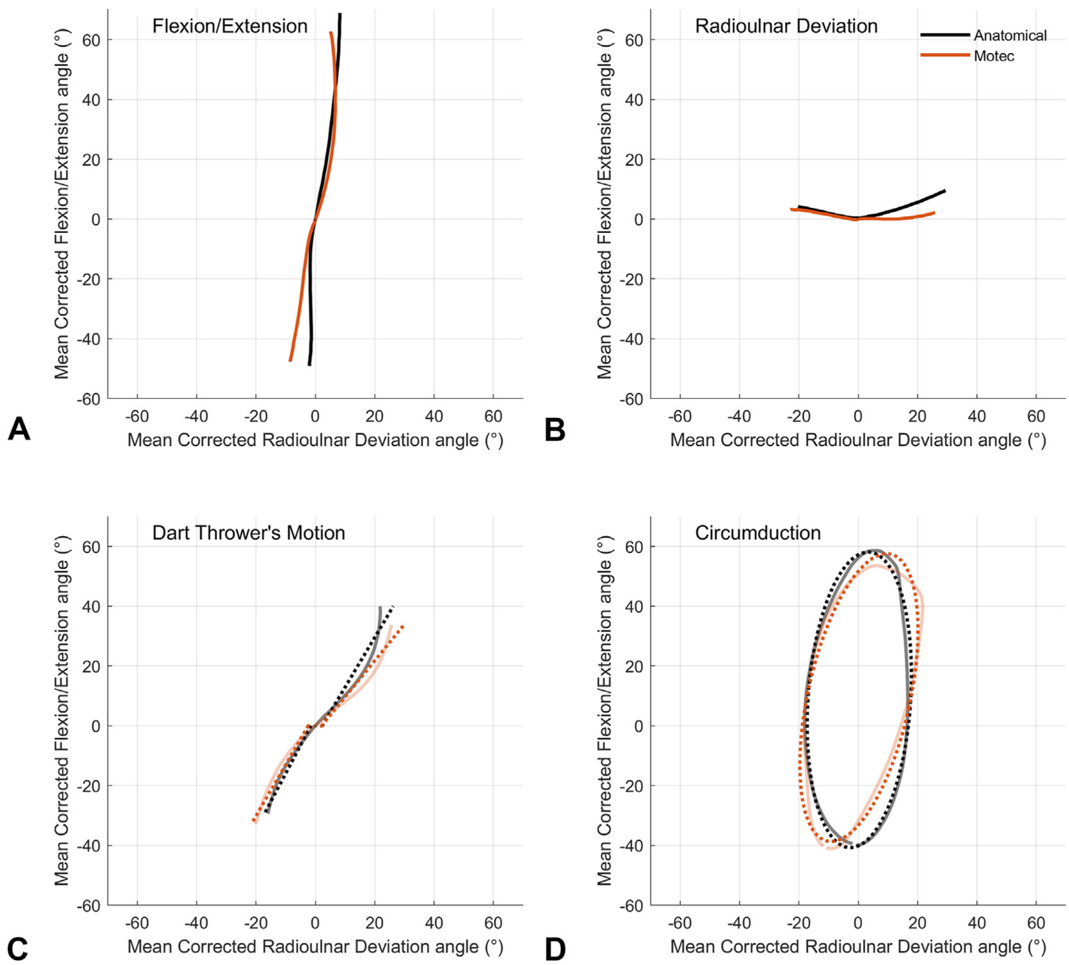

FIGURE 3: Average ROM, corrected for initial wrist position, in preoperative and postoperative wrists about the flexion (+)/extension (−) and radial (−)/ulnar (+) deviation axes of the radial coordinate system. **A** Flexion and extension (n = 14), **B** radioulnar deviation (n = 14), **C** dart-thrower's motion (n = 14), and **D** circumduction (n = 8). In **C** and **D**, regression lines fitted to the mean RE and UF profiles, and ellipses fitted to the mean circumduction profiles are plotted over the average wrist angle trajectories as dotted lines. Regression lines and ellipses fitted to individual specimen trajectories were used to calculate DTM and circumduction orientation with respect to the sagittal plane (y axis) and the circumduction area.

org). However, marked inter-specimen differences can be seen in the starting point of each motion (Figure S1, available online on the *Journal's* website at www.jhandsurg.org).

Range of motion

Figure 2 shows ROM corrected for the initial wrist position in each specimen pre- and post-TWA. Programmed motion patterns produced the required movement; however, there was marked inter-specimen variation, and out-of-plane movements were present in flexion, extension, RD, and UD (Fig. 2A, B, E, F). There were additional inter-specimen variations in the length and angle of the RE and UF trajectories and in the size of the circumduction envelope (Fig. 2C, D, G, H). Figure 3 shows the mean corrected ROM across all pre- and post-TWA wrists.

Differences in pre- and post-TWA wrist ROM in planar motions highlight potential ROM alterations after TWA implantation (Table 1). Maximum in-plane wrist angles did not significantly vary between conditions ($P > .05$). Out-of-plane angles about the y and z axes varied significantly in extension and UD, whereas angles about the x-axis varied significantly in flexion and extension ($P < .05$) (Table 1).

Orientations of RE and UF motion paths with respect to the sagittal plane (Fig. 3C) were 29.4° ± 10.1° and 30.9° ± 9.0° in the pre-TWA condition. Post-TWA, these angles increased to 30.6° ± 8.7° and 38.5° ± 9.4°, respectively. The increase was statistically significant in UF ($P < .05$), but not in RE ($P = .59$). The mean area of the circumduction ellipse (Fig. 3D) was 2533.1° ± 743.1° in anatomic wrists.

ARTICLE IN PRESS

TABLE 1. Presurgical and Postsurgical Wrist ROM (°) in Each Planar Motion

Axis of Radial Coordinate System		Wrist Angles (°)					
		Flexion	Extension	Radial Deviation	Ulnar Deviation	Radial Extension	Ulnar Flexion
x-axis	Anatomical	−1.5 ± 5.1	−1.4 ± 3.9	−3.3 ± 4.7	5.6 ± 4.3	−10.8 ± 6.5	−0.8 ± 4.3
	Motec	−4.7 ± 6.2	3.9 ± 7.4	0.0 ± 7.9	4.0 ± 7.0	−9.8 ± 12.0	−4.7 ± 7.4
	P value	<.05*	<.05*	.08	.34	.63	.07
y-axis	Anatomical	58.6 ± 11.9†	−57.7 ± 8.6†	−6.6 ± 6.1	−0.8 ± 7.2	−39.8 ± 10.6†	30.5 ± 9.3†
	Motec	55.7 ± 11.5†	−56.8 ± 8.4†	−4.6 ± 13.3	−6.2 ± 11.1	−42.4 ± 13.2†	26.1 ± 8.6†
	P value	.23†	.69†	.49	<.05*	.32	<.05*
z-axis	Anatomical	8.7 ± 4.6	−1.4 ± 6.9	−18.8 ± 7.7†	30.2 ± 4.4†	−14.3 ± 7.5†	22.2 ± 6.8†
	Motec	6.4 ± 7.0	−6.5 ± 9.1	−21.0 ± 10.9†	27.8 ± 6.1†	−18.1 ± 10.6†	27.7 ± 6.3†
	P value	.22	<.05*	.29†	.07†	<.05*	<.05*

The x-axis corresponds to pronation (+) and supination (−), the y-axis to flexion (+) and extension (−), and the z-axis to ulnar (+) and radial (−) deviation. Angles are reported as the mean ± SD.
*Indicates statistically significant differences between anatomical and Motec wrists (*P* value <.05). N = 14.
†Indicates in-plane movement (ie, the movement being replicated).

After TWA implantation, the area increased slightly to 2982.1° ± 1084.7°, although the increase was not statistically significant ($P = .11$). The orientation of the circumduction ellipse with respect to the sagittal plane was 4.9° ± 3.2° in the anatomic wrist, increasing to 12.1° ± 4.8° ($P < .05$) with the TWA. Root mean squared errors, indicating goodness of fit of the regression lines to the RE and UF paths as well as the ellipses to the circumduction envelopes, were 1.2° ± 0.7°, 2.5° ± 1.2°, and 2.9° ± 1.4°, respectively.

Peak tendon forces

Mean peak tendon forces during flexion-extension, radioulnar deviation, DTM, and circumduction are shown in Table 2. Tendon forces were either unchanged or decreased after TWA implantation. There were no statistically significant changes in peak tendon forces other than a post-implantation decrease in forces in extensor carpi ulnaris during extension, flexor carpi radialis during flexion/extension and circumduction, and flexor carpi ulnaris in all motions (Table 2).

DISCUSSION

This study suggests that the studied ball-and-socket TWA has the potential to replicate both in-plane and coupled movements of the wrist. Moreover, with a slight alteration to motion paths, it can do this efficiently with no increase in force required to replicate the movements.

Cadaveric motion was simulated in anatomic and TWA wrists by applying prescribed displacements to the five major wrist flexors and extensors, with high intra-specimen repeatability of wrist angles and tendon forces but low inter-specimen repeatability (Figure S1, available online on the *Journal's* website at www.jhandsurg.org).[13] We therefore limited our statistical analyses to presurgical and postsurgical comparisons in the same specimen.

In addition, the extent to which our cadaveric simulation represented the mechanical and physiological condition of the *in vivo* wrist was limited, as only five tendon actuators were included and neither antagonistic muscle forces nor external loading were simulated. Our cadaveric data does, however, provide a useful inference into the potential performance of this prosthesis.

In-plane wrist ROM was conserved following TWA implantation (Table 1) with our post-implantation arcs being similar to clinical results with this prosthesis, reported as 112°−120° of flexion and extension and 30°−40° of radioulnar deviation.[7,8,20] Also, our postimplantation plane and range of DTM, and circumduction ellipse areas were equal to those required to perform 70% to 90% of activities of daily living measured by Gracia-Ibáñez et al.[21] There are, to date, no published clinical reports of post-operative ranges of coupled movements with this implant.

Given the importance of DTM to activities of daily living, it is desirable that TWAs can replicate this movement.[5,18] In a study comparing healthy wrists

TABLE 2. Peak Tendon Forces (N) in Preoperative and Postoperative Wrists

Tendon		Tendon Forces (N) Flexion/Extension	Radioulnar Deviation	DTM	Circumduction
ECU	Anatomical	43.4 ± 10.4	27.1 ± 10.0	14.0 ± 7.0	30.9 ± 11.7
	Motec	34.1 ± 12.3	26.8 ± 14.2	9.7 ± 7.0	30.0 ± 11.2
	P value	<.05*	.92	.05	.85
ECRB	Anatomical	21.9 ± 9.2	7.2 ± 8.8	15.4 ± 11.1	16.2 ± 7.7
	Motec	21.6 ± 9.3	6.2 ± 5.9	14.8 ± 10.2	16.7 ± 11.3
	P value	.46	.95	.46	.90
ECRL	Anatomical	31.9 ± 6.5	45.9 ± 13.2	45.3 ± 12.4	33.0 ± 9.7
	Motec	30.3 ± 13.2	46.9 ± 19.7	42.4 ± 17.2	41.5 ± 18.2
	P value	.61	.80	.57	.13
FCR	Anatomical	39.8 ± 12.7	36.2 ± 13.8	17.7 ± 16.5	31.2 ± 10.3
	Motec	21.0 ± 6.2	31.3 ± 18.0	11.9 ± 9.9	15.3 ± 4.0
	P value	<.05*	.07	.14	<.05*
FCU	Anatomical	30.5 ± 9.1	10.9 ± 4.0	34.7 ± 9.4	30.0 ± 10.5
	Motec	13.5 ± 5.9	5.8 ± 3.0	18.6 ± 6.4	18.1 ± 8.8
	P value	<.05*	<.05*	<.05*	<.05*

Mean peak tendon force ± SD during flexion/extension (n = 14), radioulnar deviation (n = 14), dart-thrower's motion (n = 14), and circumduction (n = 8). ECRB, extensor carpi radialis brevis; ECRL, extensor carpi radialis longus; ECU, extensor carpi ulnaris; FCR, flexor carpi radialis; FCU, flexor carpi ulnaris.

*Indicates statistically significant differences between anatomical and Motec wrists (*P* value <.05).

and wrists following implantation of a Freedom prosthesis, Akhbari et al[9] showed axes of rotation during DTM to be consistent in healthy wrists but follow a complicated pattern in replaced wrists. These results imply a deficiency of the implant in replicating dart throwing planes, hypothesized as being because the Freedom, and most other current TWA implants, is designed to replicate radiocarpal rather than midcarpal kinematics.[9] Dart-thrower's motion is instead thought to arise primarily through motion at the midcarpal joint.[22,23] The ball-and-socket design of the device studied in this investigation is intended to replicate function rather than the anatomy of the wrist, and our ROM analysis indicates that this prosthesis can replicate motion in a dart throwing plane (Figs. 2, 3).

Out-of-plane motion varied between anatomical and TWA wrists in most motions (Table 1). There was also a shift in DTM and circumduction orientation. One explanation could be that the ball-and-socket is less constrained than the anatomical wrist, meaning that the "path of least resistance" is altered. Some bony constraints are eliminated by the TWA surgery, for example, the hook of the hamate is known to limit UF through impingement against the triquetrum.[24,25] It is also hypothesized that the distal carpal row is guided by the scaphoid during DTM.[25] The anatomical wrist is also stabilized by multiple carpal ligaments that support midranges and limit end ranges of motion.[26,27] Wrist motion has been demonstrated to increase following ligament sectioning in cadaveric simulation.[28] Implantation of this TWA involves a proximal row carpectomy and thus removal of many of these stabilizing anatomical structures, which may influence measured wrist motion paths. Finally, it is possible that soft tissue tension was altered between anatomic and TWA conditions. Overtensioning of soft tissues caused by the insertion of too large an implant ("over-stuffing") is thought to cause pain, stiffness, and reduced ROM *in vivo* and could have influenced wrist angle trajectories in the present study.[29]

It is unlikely that any prosthetic TWA can fully replicate the complex anatomy and mechanics of the wrist. All designs involve some compromise. In the case of ball-and-socket arthroplasties, ultimate ROM in any direction is limited by physical impingement of the neck of the head against the rim of the cup, following which levering of one against the other takes over from rotation of the head within the cup.[30] Impingement was observed during some trials in this series, but did not affect the maintenance of anatomic ROM (Table 1). Reigstad and Røkkum[12] estimated that this implant should have an impingement-free

ROM of around 70° in all directions; however, in practice, the exact range may be altered by the alignment of the screws with long axes of the radius and MCIII.

Tendon forces recorded by our simulator provide an insight into the efficiency of cadaveric wrist motion pre- and post-TWA. We found that the maximum tendon forces required to perform similar ranges of wrist motion were the same or less after TWA (Table 2), suggesting that TWA does not reduce the efficiency of the wrist. The preoperative and postoperative force comparison is a useful indicator, but these tendon forces cannot be applied directly to *in vivo* biomechanics. Antagonistic muscle forces and external loads, including gravity, which were not simulated, could result in markedly different tendon force distributions. In addition, it is possible that different stabilizing muscle forces are required after a TWA because many existing anatomical constraints have been removed.

This *in vitro* study compared the movement patterns and efficiency of the anatomic wrist with those following the insertion of a TWA. The results would suggest that this arthroplasty can accurately recreate all normal movements of the wrist, both in-plane and coupled, with good efficiency. Further studies should aim to ensure that these findings are replicated in vivo.

CONFLICTS OF INTEREST

Miss Glanville reports an unrestricted research grant from Swemac Innovations AB, the manufacturers of the Motec prosthesis, to support this project. Mr Brown reports an unrestricted research grant from Swemac Innovations AB, the manufacturers of the Motec prosthesis, to support this project; he is a paid consultant for Swemac for education and product development; he did not receive any payment for any aspects relating to this project, and receives no royalties. No benefits in any form have been received or will be received by the other authors related directly to this article.

ACKNOWLEDGMENTS

We would like to acknowledge Mr James Kennedy and Ms Harriet Julian who assisted the clinical authors in the surgical preparation of cadaveric specimens. We also thank Steph Hanna for obtaining computed tomography scans. This work was funded by the Engineering & Physical Sciences Research Council (grant no. 2439558), Swemac, the University of Liverpool and Medical Research Council and Versus Arthritis as part of the Medical Research Council Versus Arthritis Centre for Integrated Research into Musculoskeletal Ageing (grant no. MR/P020941/1). The funders had no role in study design, data collection and analysis, decision to publish, or preparation of the manuscript.

REFERENCES

1. Brigstocke G, Hearnden A, Holt CA, Whatling G. The functional range of movement of the human wrist. *J Hand Surg Eur Vol*. 2013;38(5):554−556.
2. Brumfield RH, Champoux JA. A biomechanical study of normal functional wrist motion. *Clin Orthop Relat Res*. 1984;187:23−25.
3. Palmer AK, Werner FW, Murphy D, Glisson R. Functional wrist motion: a biomechanical study. *J Hand Surg Am*. 1985;10(1):39−46.
4. Ryu JY, Cooney WP III, Askew LJ, An KN, Chao EY. Functional ranges of motion of the wrist joint. *J Hand Surg Am*. 1991;16(3):409−419.
5. Moritomo H, Apergis EP, Herzberg G, Werner FW, Wolfe SW, Garcia-Elias M. 2007 IFSSH committee report of wrist biomechanics committee: biomechanics of the so-called dart-throwing motion of the wrist. *J Hand Surg Am*. 2007;32(9):1447−1453.
6. Moritomo H, Apergis EP, Garcia-Elias M, Werner FW, Wolfe SW. International Federation of Societies for Surgery of the Hand 2013 Committee's report on wrist dart-throwing motion. *J Hand Surg Am*. 2014;39(7):1433−1439.
7. Berber O, Garagnani L, Gidwani S. Systematic review of total wrist arthroplasty and arthrodesis in wrist arthritis. *J Wrist Surg*. 2018;7(5):424−440.
8. Eschweiler J, Li J, Quack V, et al. Total wrist arthroplasty-a systematic review of the outcome, and an introduction of freemove-an approach to improve TWA. *Life (Basel)*. 2022;12(3):411.
9. Akhbari B, Morton AM, Shah KN, et al. Proximal-distal shift of the center of rotation in a total wrist arthroplasty is more than twice of the healthy wrist. *J Orthop Res*. 2020;38(7):1575−1586.
10. Hooke AW, Pettersson K, Sagerfors M, An KN, Rizzo M. An anatomic and kinematic analysis of a new total wrist arthroplasty design. *J Wrist Surg*. 2015;4(2):121−127.
11. Bjarnason JA, Reikeras O. Changes of center of rotation and femoral offset in total hip arthroplasty. *Ann Transl Med*. 2015;3(22):355.
12. Reigstad O, Røkkum M. Wrist arthroplasty using prosthesis as an alternative to arthrodesis: design, outcomes and future. *J Hand Surg Eur Vol*. 2018;43(7):689−699.
13. Glanville J, Bates K, Brown D, Potts D, Curran J, Fichera S. Evaluation of a cadaveric wrist motion simulator using marker-based x-ray reconstruction of moving morphology. *PeerJ*. 2024;12:e17179.
14. Tang JB, Giddins G. Why and how to report surgeons' levels of expertise. *J Hand Surg Eur Vol*. 2016;41(4):365−366.
15. Brainerd EL, Baier DB, Gatesy SM, et al. X-ray reconstruction of moving morphology (XROMM): precision, accuracy and applications in comparative biomechanics research. *J Exp Zool A Ecol Genet Physiol*. 2010;313(5):262−279.
16. Knörlein BJ, Baier DB, Gatesy SM, Laurence-Chasen JD, Brainerd EL. Validation of XMALab software for marker-based XROMM. *J Exp Biol*. 2016;219(23):3701−3711.
17. Akhbari B, Moore DC, Laidlaw DH, et al. Predicting carpal bone kinematics using an expanded digital database of wrist carpal bone anatomy and kinematics. *J Orthop Res*. 2019;37(12):2661−2670.
18. Brigstocke GHO, Hearnden A, Holt C, Whatling G. In-vivo confirmation of the use of the dart thrower's motion during activities of daily living. *J Hand Surg Eur Vol*. 2014;39(4):373−378.
19. Garg R, Kraszewski AP, Stoecklein HH, et al. Wrist kinematic coupling and performance during functional tasks: effects of constrained motion. *J Hand Surg Am*. 2014;39(4):634−642.e1.
20. Giwa L, Siddiqui A, Packer G. Motec wrist arthroplasty: 4 years of promising results. *J Hand Surg Asian Pac Vol*. 2018;23(3):364−368.

ARTICLE IN PRESS

21. Gracia-Ibáñez V, Sancho-Bru JL, Vergara M, Roda-Sales A, Jarque-Bou NJ, Bayarri-Porcar V. Biomechanical function requirements of the wrist. Circumduction versus flexion/abduction range of motion. *J Biomech*. 2020;110:109975.
22. Werner FW, Green JK, Short WH, Masaoka S. Scaphoid and lunate motion during a wrist dart throw motion. *J Hand Surg Am*. 2004;29(3):418−422.
23. Crisco JJ, Coburn JC, Moore DC, Akelman E, Weiss AC, Wolfe SW. In vivo radiocarpal kinematics and the dart thrower's motion. *J Bone Joint Surg Am*. 2005;87(12):2729−2740.
24. Kamal RN, Rainbow MJ, Akelman E, Crisco JJ. In vivo triquetrum-hamate kinematics through a simulated hammering task wrist motion. *J Bone Joint Surg Am*. 2012;94(12):e85.
25. Edirisinghe Y, Troupis JM, Patel M, Smith J, Crossett M. Dynamic motion analysis of dart throwers motion visualized through computerized tomography and calculation of the axis of rotation. *J Hand Surg Eur Vol*. 2014;39(4):364−372.
26. Rainbow MJ, Kamal RN, Moore DC, Akelman E, Wolfe SW, Crisco JJ. Subject-specific carpal ligament elongation in extreme positions, grip, and the dart thrower's motion. *J Biomech Eng*. 2015;137(11):111006.
27. Tang JB, Gu XK, Xu J, Gu JH. In vivo length changes of carpal ligaments of the wrist during dart-throwing motion. *J Hand Surg Am*. 2011;36(2):284−290.
28. Badida R, Akhbari B, Vutescu E, Moore DC, Wolfe SW, Crisco JJ. The role of scapholunate interosseous, dorsal intercarpal, and radio-lunate ligaments in wrist biomechanics. *J Biomech*. 2021;125:110567.
29. Redfern J, Mehta N, Farnebo S, et al. Complication rates and modes of short and medium-term failure in Motec total wrist arthroplasty: an international cohort study. *J Hand Surg Eur Vol*. 2024;49(1):27−33.
30. Kandemir G, Julian H, Joyce T, Brown D. Investigation of the in vivo performance of metal-on-metal motec total wrist arthroplasty—an explant analysis. *J Wrist Surg*. Published online May 23, 2024. https://doi.org/10.1177/17531934241249919